PHILOSOPHICAL TRANSACTIONS OF THE ROYAL SOCIETY A MATHEMATICAL, PHYSICAL & ENGINEERING SCIENCES

On the Structure of Tilt Grain Boundaries in Cubic Metals II. Asymmetrical Tilt Boundaries

A. P. Sutton and V. Vitek

Phil. Trans. R. Soc. Lond. A 1983 **309**, 37-54
doi: 10.1098/rsta.1983.0021

Phil. Trans. R. Lond. A **309**, 37–54 (1983) [37]
Printed in Great Britain

ON THE STRUCTURE OF TILT GRAIN BOUNDARIES IN CUBIC METALS II. ASYMMETRICAL TILT BOUNDARIES

By A. P. SUTTON† and V. VITEK
Department of Materials Science and Engineering and the Laboratory for Research on the Structure of Matter, University of Pennsylvania, Philadelphia, Pennsylvania 19104, *U.S.A.*

(*Communicated by J. W. Christian, F.R.S. – Received* 1 *April* 1982)

CONTENTS

The results of the study of symmetrical tilt boundaries, reported in the preceding part I, are generalized to asymmetrical tilt boundaries. A classification of tilt boundaries in cubic crystals is developed that reveals which boundaries to choose in order to study equilibrium faceting or intrinsic grain boundary dislocations (g.b.ds) accommodating a misorientation. Two series of atomistic studies of asymmetrical tilt boundary structures are presented based on this classification.

The first is a study of long-period ($\Sigma \leqslant 97$) $[1\bar{1}0]$ asymmetrical tilt boundaries in aluminium. The aims of this study are to investigate whether these boundaries are composed of fundamental structural elements, in the same way as was found in part I for symmetrical tilt boundaries, and to see if localized, distinct stress fields of edge g.b.ds exist throughout the misorientation range. With use of the results of this study, and the principle of continuity of boundary structure enunciated in part I, the boundary unit representation of a $\Sigma = 1193$ asymmetrical tilt boundary is derived as an example. It is generally found that the Burgers vectors of intrinsic secondary g.b.ds in tilt boundaries, based on favoured boundary reference structures, are non-primitive d.s.c. vectors. The reason for this is given and a simple formula is presented to derive the Burgers vectors of such dislocations for any favoured tilt boundary reference structure. It is pointed out that, in general, very low angle ($\theta < 1°$ say) tilt boundaries cannot be described in terms of units from high angle tilt boundaries, and the transition from the low angle to high angle régimes is discussed.

The second atomistic study is an investigation of equilibrium faceting of long-period $\Sigma = 3[1\bar{1}0]$ tilt boundaries with use of an empirical potential for copper. The limi-

† Present address: Department of Metallurgy and Science of Materials, University of Oxford, Parks Road, Oxford OX1 3PH, U.K.

tations of computer simulation methods using periodic border conditions to study faceting are stated. It is shown, however, that the constraints imposed by the use of periodic border conditions may be used in a positive sense to carry out the Wulff construction, and thereby deduce equilibrium faceting behaviour.

1. Introduction

In this paper the results of the study of symmetrical tilt boundaries, reported in the preceding part I, are generalized to asymmetrical tilt boundaries. By an asymmetrical tilt boundary we mean a tilt boundary in which the crystal planes parallel to the interface in both grains are not of the same crystallographic form: for example $(225)_1/(441)_2$ is asymmetrical while $(116)_1/(\bar{1}\bar{1}6)_2$ is symmetrical. Asymmetrical tilt boundaries have one degree of freedom more than symmetrical tilt boundaries, i.e. the boundary inclination may be varied at constant misorientation between the adjoining grains. Thus for a given misorientation an infinite number of boundaries exist in principle but in equilibrium most of them may facet into a few low energy boundaries.

As will be discussed in §3.3 macroscopic faceting cannot be simulated by atomistic calculations when periodic border† conditions are used. When the facets are sufficiently small they may be described as steps on the dominant boundary plane. There are two types of step that may exist (Hirth & Balluffi 1973). The first is a perfect step (Ashby 1972), which is not associated with a dislocation, and the step vector (King & Smith 1980) is in this case a (coincidence site lattice) c.s.l. vector. An interface containing such steps is free of long-range stresses (Hirth & Balluffi 1973, Christian & Knowles 1981). This is the type of boundary that is produced during equilibrium faceting of an embedded grain at high temperatures. The second type of step is associated with a dislocation, and the step vector is not a c.s.l. vector. An interface containing such steps does have a long-range stress field. For example, the curved interface of a lenticular deformation twin contains twinning dislocations, which are associated with steps, on the coherent twin boundary plane. The long-range stress field of such an interface may be relaxed by emission or absorption of lattice dislocations, which annihilate dislocations associated with the steps (see for example Sleeswyk 1962).

In a computer simulation of the atomic structure of a tilt boundary it is clear that if there is any tendency for the boundary to facet it can do so only by the creation of perfect steps. The reason is that the border conditions imposed require zero stresses far from the boundary. Thus in the atomistic study of faceting presented below we shall only be able to discuss equilibrium faceting, which involves the creation of perfect steps.

Two series of atomistic calculations of asymmetrical tilt boundary structures are presented and analysed in §3. The methods of calculation and interpretation of the results, and the interatomic potentials were described in part I. However, it is first necessary to explain how the boundaries used in these studies were selected since this is not obvious *a priori*. A geometrical classification of tilt boundaries in cubic crystals is developed in §2 that indicates which tilt boundaries to choose to study equilibrium faceting or secondary, intrinsic edge (grain boundary dislocation) g.b.d. formation. The results of the atomistic calculations are then readily understood and generalized within the framework of this geometrical classification.

† By border conditions we mean the conditions imposed on the faces of the computational cell perpendicular to the boundary plane. We have not used 'boundary conditions' to avoid confusion with conditions imposed on the grain boundary such as the necessity for it to be periodic.

2. Geometrical classification of tilt boundaries in cubic crystals

In the following classification it is assumed that if the indices of the local boundary plane are different from those of the macroscopic boundary plane then such variations are effected by the introduction of only whole units of the corresponding boundaries. Thus imperfect steps, such as those associated with twinning dislocations, are excluded. It is also assumed that steps are not associated with intrinsic secondary g.b.ds in tilt boundaries that accommodate a misorientation from some favoured boundary, and that their Burgers vectors are normal to the favoured boundary plane. The latter assumption is supported by the atomistic calculations reported in §3.2 and arguments presented recently by King & Smith (1980) and King (1982) indicating that steps associated with intrinsic g.b.ds accommodating a misorientation are, in general, energetically unfavourable. Thus local changes in misorientation and inclination are assumed to occur independently through step-less edge g.b.ds with Burgers vector normal to the reference boundary plane and dislocation free steps, respectively.

To discuss secondary, intrinsic g.b.d. formation we consider all possible tilt boundaries in which the upper and lower grains are obtained by rotations of plus and minus $\frac{1}{2}\theta$ respectively, from some plane in the ideal crystal containing the tilt axis, where θ is the angle of misorientation across the resulting boundary. For definiteness we shall consider $[1\bar{1}0]$ tilt boundaries, but the procedure is readily generalized to other tilt axes. Let the atomic plane in the ideal crystal, from which the boundaries are derived, be called the mean boundary plane and let its indices be $(h_s h_s k_s)$. Consider the lattice with basis vectors $\frac{1}{2}[1\bar{1}0]$, $f_1[h_s h_s k_s]$ and $f_2[k_s k_s \overline{2h_s}]$ where f_1 and f_2 are the appropriate cell factors for the crystal Bravais lattice (Christian 1975). This lattice, which is illustrated in figure 1, is a sub-lattice of the median lattice, and the volume of its primitive cell is $(2h_s^2 + k_s^2) f_1 f_2$. In figure 1 the positive tilt axis is normal to the page pointing towards the reader. Let $\boldsymbol{p}_1$ and $\boldsymbol{p}_2$ be the period vectors in the upper and lower grains, respectively, of a periodic boundary that we shall obtain from the lattice shown in figure 1. Similarly, let $\boldsymbol{n}_1$ and $\boldsymbol{n}_2$ be the unit normals of the boundary plane with respect to the upper and lower grains where, by convention, $\boldsymbol{n}_1$ and $\boldsymbol{n}_2$ both point from the lower to the upper grain. To ensure $|\boldsymbol{p}_1| = |\boldsymbol{p}_2|$, and therefore that the boundary is periodic, we write

$$\boldsymbol{p}_1 = xf_2[k_s k_s \overline{2h_s}] + yf_1[h_s h_s k_s], \quad \boldsymbol{p}_2 = xf_2[k_s k_s \overline{2h_s}] - yf_1[h_s h_s k_s], \tag{1}$$

where x and y are positive integers. In figure 1 $(x, y) = (3, 1)$. The coordinate frame shown in figure 1 is affixed to both upper ($y > 0$) and lower ($y < 0$) grains and the infinite wedge of ideal crystal between the $\boldsymbol{p}_1$ and $\boldsymbol{p}_2$ directions is removed. The upper grain is then rotated by $\frac{1}{2}\theta$ in an anticlockwise sense about the positive tilt axis and the lower grain by $\frac{1}{2}\theta$ in the opposite sense. The two grains now meet in the plane $y = 0$ of figure 1 and they are welded together to form a grain boundary. Although $\boldsymbol{p}_1$, $\boldsymbol{p}_2$ and $\boldsymbol{n}_1$, $\boldsymbol{n}_2$ are parallel it must be remembered that the upper and lower grain coordinate frames are now misoriented by θ, and that the components of $\boldsymbol{p}_1$ and $\boldsymbol{p}_2$ are still given by equations (1). By allowing x and y to assume any positive integer values we may thus construct all periodic boundaries obtainable by rotations of $\pm\frac{1}{2}\theta$ from $(h_s h_s k_s)$ of the ideal crystal. Irrational boundaries may be represented to any required accuracy by allowing x and y to assume infinite values. Adding the components of $\boldsymbol{p}_1$ and $\boldsymbol{p}_2$ we obtain a vector that is always parallel to $[k_s k_s \overline{2h_s}]$ of figure 1. Since $[k_s k_s \overline{2h_s}]$ is also parallel to the period vectors $\boldsymbol{p}_1$ and $\boldsymbol{p}_2$ after the boundary is formed we call $\frac{1}{2}(\boldsymbol{p}_1 + \boldsymbol{p}_2)$ the mean period vector. Similarly, by adding the components of $\boldsymbol{n}_1$ and $\boldsymbol{n}_2$ we always obtain a vector that is parallel to $[h_s h_s k_s]$ of figure 1, which is,

of course, the normal to the mean boundary plane $(h_s h_s k_s)$. Hence all boundaries created in this manner share the same mean boundary plane and their mean period vectors are parallel. For any tilt axis the mean boundary plane must lie in the zone of the tilt axis so it may always be characterized by a single parameter, which we call ξ. We choose $\xi = k_s/h_s$ to characterize the mean boundary plane $(h_s h_s k_s)$, and all boundaries sharing this mean boundary plane are said to belong to the same ξ-system. As we shall see in § 3.2 the physical significance of a ξ-system is that secondary intrinsic g.b.d. formation in a long-period tilt boundary corresponds to the introduction of units of favoured boundaries from within the same ξ-system. Thus, once all the

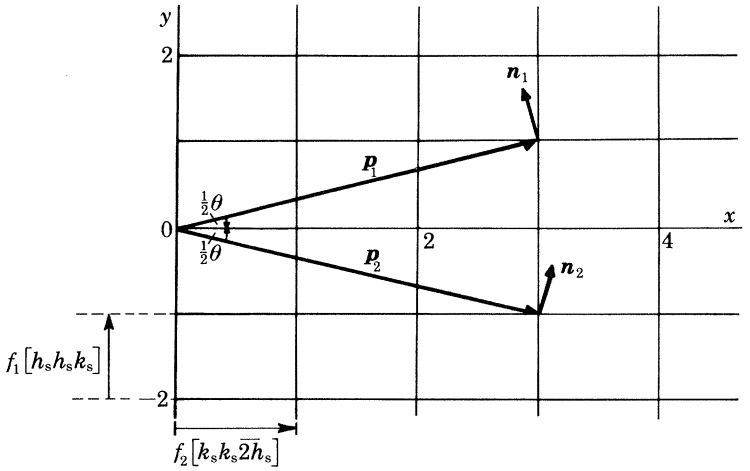

FIGURE 1. Illustration of the construction of a $[1\bar{1}0]$ tilt boundary with upper and lower grain period vectors, $\boldsymbol{p}_1$ and $\boldsymbol{p}_2$, that are lattice vectors of the two-dimensional lattice with basis vectors $f_2[k_s k_s \overline{2}h_s]$ and $f_1[h_s h_s k_s]$. Vectors $\boldsymbol{n}_1$ and $\boldsymbol{n}_2$ will be the boundary plane normals, in the upper and lower grains, after the boundary is formed.

favoured boundaries in a ξ-system are determined the structures of all non-favoured boundaries in the ξ-system are readily deduced, if continuity of boundary structure exists throughout the misorientation ranges between the adjacent favoured boundaries, and all boundaries considered are stable with respect to faceting. The broader physical significance of a ξ-system is that all five macroscopic parameters of tilt boundaries belonging to a particular ξ-system are the same, except the misorientation, θ. Therefore, in a study of the variation of some property of tilt boundaries (such as energy, sliding rate, diffusivity etc.) with θ, one should compare only boundaries belonging to the same ξ-system.

From figure 1 we see that $\tan\frac{1}{2}\theta = yf_1/xf_2\sqrt{2}$. It follows that the reciprocal density of coincidence sites, Σ, of the coincidence system to which the tilt boundary belongs is given by $\Sigma = \mathrm{d}_2(2x^2f_2^2 + y^2f_1^2)$, where d_2 is an operator such that $\mathrm{d}_2(z)$ signifies that z is repeatedly multiplied or divided by two until z is an odd integer ($2x^2f_2^2 + y^2f_1^2$ may be fractional if f_1 and f_2 are fractional). Alternatively, by interchanging the axes of figure 1, and reversing the direction of the positive $[1\bar{1}0]$ axis, we could have created exactly the same set of boundaries but the mean period vector would have been $f_1[h_s h_s k_s]$ and the mean boundary plane would have been $(k_s k_s \overline{2}h_s)$. In that case $\tan\frac{1}{2}\theta = yf_2\sqrt{2}/xf_1$ and $\Sigma = \mathrm{d}_2(x^2f_1^2 + 2y^2f_2^2)$. In simple cubic crystals ($f_1 = 1, f_2 = 1$) these expressions reduce to those given by Ranganathan (1966). All boundaries thus manufactured from the lattice depicted in figure 1 have the same mean boundary plane

but different values of Σ. The exceptions are $\theta = 0$ and $\theta = 180°$ ($\Sigma = 1$), which is a trivial consequence of twofold rotational symmetry along $[1\bar{1}0]$.

We name the orthogonal crystal vectors, $f_1[h_s h_s k_s]$ and $f_2[k_s k_s \overline{2h_s}]$, used to construct all boundaries belonging to $\xi = k_s/h_s$, basis vectors of the ξ-system for the corresponding Bravais crystal lattice. It is essential to show first that a grain boundary, in a particular Bravais crystal lattice, can be assigned uniquely to a ξ-system. Let $\boldsymbol{a}_1$, $\boldsymbol{a}_2$ be basis vectors for the ξ_a system and $\boldsymbol{b}_1$, $\boldsymbol{b}_2$ be basis vectors for the ξ_b system. Suppose that a boundary with upper and lower grain period vectors, $\boldsymbol{p}_1$ and $\boldsymbol{p}_2$, can be assigned to both ξ systems. Then

$$\boldsymbol{p}_1 = x\boldsymbol{a}_1 + y\boldsymbol{a}_2 = r\boldsymbol{b}_1 + q\boldsymbol{b}_2, \quad \boldsymbol{p}_2 = x\boldsymbol{a}_2 - y\boldsymbol{a}_2 = r\boldsymbol{b}_1 - q\boldsymbol{b}_2,$$

where x, y, r, q are positive integers. By adding and subtracting these equations we deduce $x\boldsymbol{a}_1 = r\boldsymbol{b}_1$ and $y\boldsymbol{a}_2 = q\boldsymbol{b}_2$. Therefore $\boldsymbol{a}_1$ and $\boldsymbol{b}_1$ are parallel, as are $\boldsymbol{a}_2$ and $\boldsymbol{b}_2$, and hence $\xi_a = \xi_b$. However, although a boundary may be assigned uniquely to a ξ-system there are equivalent ξ-systems. Equivalent ξ-systems are related by crystal symmetry operations on the coordinate system of the ideal crystal before the boundary is formed. In addition, we have already seen that the same set of boundaries is generated if the basis vectors $f_1[h_s h_s k_s]$ and $f_2[k_s k_s \overline{2h_s}]$ are exchanged. Therefore, $\xi = k_s/h_s$ is equivalent to $\xi = -2h_s/k_s$. Similarly, if $f_1[\bar{h}_s \bar{h}_s k_s]$ and $f_2[k_s k_s 2h_s]$ had been used as basis vectors, a one-to-one equivalence would be found between the structures of boundaries in the two ξ-systems k_s/h_s and $-k_s/h_s$ and hence the following ξ-systems are equivalent in $[1\bar{1}0]$ tilt boundaries: k_s/h_s, $-k_s/h_s$, $2h_s/k_s$, $-2h_s/k_s$.

Symmetrical tilt boundaries either have a mean boundary plane that is a crystal mirror plane or their mean period vector is an even-fold rotation axis of the ideal crystal. In cubic crystals {110} and {001} are mirror planes and ⟨110⟩ and ⟨001⟩ are even-fold rotation axis. At least one of the conditions for symmetrical tilt boundaries can be satisfied if the tilt axis lies in a ⟨100⟩ or ⟨110⟩ zone. This observation has also been made by Fortes (1972). The lowest-index tilt axis that does not allow symmetrical tilt boundaries is thus ⟨123⟩. The $[1\bar{1}0]$ symmetrical tilt boundaries studied in part I, §4 all have mean boundary plane normals of the upper and lower grains listed in tables 1 and 2 of part I. Similarly, the symmetrical [001] tilt boundaries studied in part I, §5 have mean boundary plane (110) and mean period vector $[\bar{1}10]$. Finally the $[11\bar{1}]$ symmetrical tilt boundaries studied in part I, §6 have mean boundary plane $(1\bar{1}0)$ and mean period vector [112].

To illustrate the use of equation (1) to generate asymmetrical $[1\bar{1}0]$ tilt boundaries within the same ξ-system consider the $\xi = 1$ system in f.c.c. crystals. In this case $k_s/h_s = 1$ so we choose $k_s = 1$, $h_s = 1$ corresponding to a mean boundary plane (111) and mean period vector $\frac{1}{2}[11\bar{2}]$ ($f_1 = 1, f_2 = \frac{1}{2}$). This is the lowest-index mean boundary plane that will generate asymmetrical $[1\bar{1}0]$ tilt boundaries. Equations (1) become

$$\boldsymbol{p}_1 = \tfrac{1}{2}x[11\bar{2}] + y[111], \quad \boldsymbol{p}_2 = \tfrac{1}{2}x[11\bar{2}] - y[111]. \tag{2}$$

A boundary in which $\boldsymbol{p}_1$ and $\boldsymbol{p}_2$ are given by equations (2) may be represented by the ordered pair (x, y) and it belongs to the coincidence systems $\Sigma = x^2 + 2y^2$. Table 1 lists some of the boundaries in $\xi = 1$ system. Note that in some cases the period vectors and boundary planes are expressed as multiples of crystal vectors and crystal planes, e.g. $\boldsymbol{p}_1 = \frac{1}{2}[330]_1$ and $(003)_1$ in the case of the boundary (1, 1). This is done to ensure that $|\boldsymbol{p}_1| = |\boldsymbol{p}_2|$, $\boldsymbol{p}_1 + \boldsymbol{p}_2$ is parallel to $[11\bar{2}]$ and the sum of the boundary plane normals is parallel to [111]. Of course, when the boundary plane is expressed as $(003)_1$ it is understood that the atomic plane parallel to the boundary in the

upper grain is $(002)_1$. The boundaries (1, 1) to (1, 2), listed in table 1, are the subject of an atomistic study reported in § 3.

We now turn to considerations of faceting of tilt boundaries. Consider an embedded prism grain with the rotation axis parallel to the prism axis. The prism faces that are parallel to the prism axis will then be tilt boundaries. The possible tilt boundary planes of such a faceted prism grain may again be generated on the basis of equations (1). In the case of faceting Σ remains constant but ξ changes from one boundary facet to another. Therefore, to describe faceting we rewrite equations (1) as follows:

$$\boldsymbol{p}_1 = h_s g_1[yy\overline{2x}] + k_s g_2[xxy], \quad \boldsymbol{p}_2 = h_s g_1[\bar{y}\bar{y}\,\overline{2x}] + k_s g_2[xx\bar{y}], \tag{3}$$

TABLE 1

boundary	$\boldsymbol{p}_1$	$\boldsymbol{p}_2$	plane	θ/deg	Σ
(1, 0)	$\frac{1}{2}[11\bar{2}]_1$	$\frac{1}{2}[11\bar{2}]_2$	$(111)_1/(111)_2$	0	1
(3, 1)	$\frac{1}{2}[55\bar{4}]_1$	$\frac{1}{2}[11\bar{8}]_2$	$(225)_1/(441)_2$	50.48	11
(5, 2)	$\frac{1}{2}[99\bar{6}]_1$	$\frac{1}{2}[1, 1, \bar{14}]_2$	$(339)_1/(771)_2$	58.99	33
(2, 1)	$[22\bar{1}]_1$	$[00\bar{3}]_2$	$(114)_1/(330)_2$	70.53	3
(3, 2)	$\frac{1}{2}[77\bar{2}]_1$	$\frac{1}{2}[\bar{1}, \bar{1}, \bar{10}]_2$	$(117)_1/(55\bar{1})_2$	86.63	17
(1, 1)	$\frac{1}{2}[330]_1$	$\frac{1}{2}[\bar{1}, \bar{1}, \bar{4}]_2$	$(003)_1/(22\bar{1})_2$	109.47	3
(5, 6)	$\frac{1}{2}[17, 17, 2]_1$	$\frac{1}{2}[\bar{7}, \bar{7}, \bar{22}]_2$	$(\bar{1}, \bar{1}, 17)_1\ (11, 11, \bar{7})_2$	118.98	97
(3, 4)	$\frac{1}{2}[11, 11, 2]_1$	$\frac{1}{2}[\bar{5}, \bar{5}, \bar{14}]_2$	$(\bar{1}, \bar{1}, 11)_1/(77\bar{5})_2$	124.12	41
(2, 3)	$[441]_1$	$[\bar{22}5]_2$	$(\bar{1}\bar{1}8)_1/(55\bar{4})_2$	129.52	11
(1, 2)	$\frac{1}{2}[552]_1$	$\frac{1}{2}[\bar{33}6]_2$	$(\bar{1}\bar{1}5)_1/(33\bar{3})_2$	141.06	9
(1, 3)	$\frac{1}{2}[774]_1$	$\frac{1}{2}[\bar{55}8]_2$	$(\bar{2}\bar{2}7)_1/(44\bar{5})_2$	153.47	19
(0, 1)	$[111]_1$	$[\bar{1}\bar{1}1]_2$	$(\bar{1}\bar{1}2)_1/(11\bar{2})_2$	180	1

where $g_1[yy\overline{2x}]$ and $g_2[xxy]$ are primitive vectors of the crystal Bravais lattice. The numbers x and y are now restricted to being coprime integers and we may construct the period vectors of all $[1\bar{1}0]$ tilt boundaries belonging to the coincidence system $\Sigma = 2x^2 + y^2$ by allowing h_s and k_s to take on any positive integer values. We use now the ordered pair $[h_s, k_s]$ to denote a boundary, the period vectors of which are given by equations (3). By adding equations (3) it is found that the mean period vector of $[h_s, k_s]$ is parallel to $[k_s g_2, k_s g_2, -2h_s g_1]$, and the mean boundary plane is parallel to $(h_s g_1, h_s g_1, k_s g_2)$. Thus the boundary $[h_s, k_s]$ belongs to the $\xi = k_s g_2/h_s g_1$ system. The upper grain period vectors of all $[1\bar{1}0]$ tilt boundaries belonging to the $\Sigma = 2x^2 + y^2$ coincidence system may thus be represented as lattice vectors of the two-dimensional lattice with basis vectors $g_1[yy\overline{2x}]$ and $g_2[xxy]$. Of course, the lower grain period vectors may be represented similarly. The basis vectors of this lattice are the $\boldsymbol{p}_1$ vectors of the two symmetrical tilt boundaries that appear in this coincidence system. That is because the basis vectors correspond to the boundaries [1, 0] and [0, 1] with mean boundary planes (110) and (001). It is therefore possible, though not necessarily energetically favourable, for all asymmetrical ⟨110⟩ tilt boundaries in a particular coincidence system to facet into the corresponding two symmetrical tilt boundaries.

To illustrate the use of equations (3) to construct all $[1\bar{1}0]$ tilt boundaries in a particular coincidence system in f.c.c. crystals we shall consider $\Sigma = 11$, for which $x = 1$, $y = 3$ or $x = 3$, $y = 2$. These two choices for x and y lead to $\theta = 129.52°$ and $\theta = 50.48°$ respectively, which are equivalent in the sense that the same set of boundary structures will be generated. Therefore we choose arbitrarily $x = 1$, $y = 3$ and then equations (3) become

$$\boldsymbol{p}_1 = \tfrac{1}{2}h_s[33\bar{2}] + k_s[113], \quad \boldsymbol{p}_2 = \tfrac{1}{2}h_s[\bar{3}\bar{3}\,\overline{2}] + k_s[11\bar{3}], \tag{4}$$

since $g_1 = \frac{1}{2}$, $g_2 = 1$. The mean boundary plane of the boundary $[h_s, k_s]$ is parallel to $(h_s h_s 2k_s)$ and it therefore belongs to the $\xi = 2k_s/h_s$ system. For b.c.c. crystals equations (4) are replaced by

$$\boldsymbol{p}_1 = h_s[33\bar{2}] + \tfrac{1}{2}k_s[113], \quad \boldsymbol{p}_2 = h_s[\bar{3}\bar{3}2] + \tfrac{1}{2}k_s[11\bar{3}],$$

since $g_1 = 1$, $g_2 = \frac{1}{2}$. In this case the boundary $[h_s, k_s]$ belongs to the $\xi = k_s/2h_s$ system.

3. Atomistic calculations of asymmetrical tilt boundaries

3.1. *Introduction*

Two series of calculations have been made that are based on the classification of tilt boundaries, presented in § 2. The first is a study of some of the boundaries belonging to the $\xi = 1$ system in aluminium. This system corresponds to the lowest-index mean boundary plane, (111), for which asymmetrical tilt boundaries exist. The aim of these calculations was to investigate whether the stress fields of localized, distinct g.b.ds exist in those asymmetrical tilt boundaries. The second series is a study of faceting in the $\Sigma = 3$ coincidence system. This is the lowest value of Σ (apart from $\Sigma = 1$) that exists and it was hoped that each boundary facet would therefore not decompose into units of boundaries in the same ξ-system. These calculations were made with use of the potential for copper. The reason why the potential for aluminium was not used in this study is explained below.

3.2. *The $\xi = 1$ system in aluminium*

Table 2 lists the boundaries selected for this study. They are from the $\theta = 109.47°$ to $\theta = 141.06°$ range of the boundaries listed in table 1. As shown below the $\Sigma = 3$ and $\Sigma = 9$ boundaries are favoured. It is proved in the Appendix that in any periodic grain boundary the odd/even form of the indices of the boundary plane with respect to the upper and lower grains is the same. Furthermore, in every boundary period, the number of crystal periods parallel to the boundary, in either grain, is always an odd integer. It follows that if the boundary plane, with respect to one grain of a $[1\bar{1}0]$ tilt boundary, has a centering site, then so does the boundary plane with respect to the other grain and therefore the boundary is centred. Thus centred $[1\bar{1}0]$ asymmetrical tilt boundaries occur when the indices of the boundary plane with respect to the upper and lower grains are all odd, and the centering site is again at the centre of the repeat cell. The vector characterizing a unit of a centred, asymmetrical $[1\bar{1}0]$ tilt boundary is therefore half the period vector in both grains. For example, the $\Sigma = 9\,(\bar{1}\bar{1}5)_1/(33\bar{3})_2$ boundary is centred and its unit is characterized by the vector $\frac{1}{4}[552]_1/\frac{1}{4}[\bar{3}\bar{3}6]_2$. We call a unit of the $\Sigma = 3$ boundary A and one of the $\Sigma = 9$ boundary B; their structures are therefore represented by |A| and |B.B| as shown in column 5 of table 2.

Table 2

boundary plane	θ/deg	Σ	period vectors	structure
$(003)_1/(22\bar{1})_2$	109.47	3	$\frac{1}{2}[330]_1/\frac{1}{2}[\bar{1}\bar{1}4]_2$	|A|
$(\bar{1}, \bar{1}, 17)_1/(11, 11, \bar{7})_2$	118.98	97	$\frac{1}{2}[17, 17, 2]_1/\frac{1}{2}[\bar{7}, \bar{7}, \bar{2}\bar{2}]_2$	|AAB.AAB|
$(\bar{1}, \bar{1}, 11)_1/(77\bar{5})_2$	124.12	41	$\frac{1}{2}[11, 11, 2]_1/\frac{1}{2}[\bar{5}, \bar{5}, \bar{1}\bar{4}]_2$	|AB.AB|
$(\bar{1}, \bar{1}, 8)_1/(55\bar{4})_2$	129.52	11	$[441]_1/[\bar{2}\bar{2}5]_2$	|AAB|
$(\bar{1}\bar{1}5)_1/(33\bar{3})_2$	141.06	9	$\frac{1}{2}[552]_1/\frac{1}{2}[\bar{3}\bar{3}6]_2$	|B.B|

Figure 2 shows the relaxed structure of the $\Sigma = 3$ boundary, which has been calculated previously by Pond & Vitek (1977). A suitable boundary unit, occupying one period of the boundary, is outlined at the boundary. The coordinate system is shown in figure 2. (111) planes

PHILOSOPHICAL TRANSACTIONS OF THE ROYAL SOCIETY A MATHEMATICAL, PHYSICAL & ENGINEERING SCIENCES

in each grain are indicated in figure 2 and it is seen that they are both inclined by 54.74° to the boundary. This shows that the boundary may indeed be regarded as a 109.47° rotation symmetrically imposed on the (111) plane of the ideal crystal. From Frank's formula we see that such a misorientation can be achieved by formally associating a lattice dislocation, of Burgers vector 2[111], with every unit of the boundary. Three (111) plane terminations can be seen at every unit in each grain, which is consistent with this formal description.

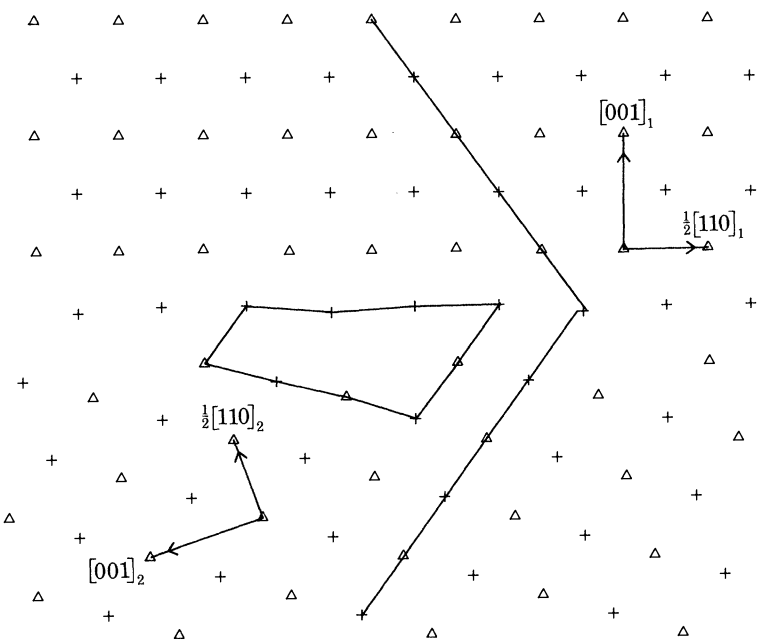

FIGURE 2. Relaxed structure of $\Sigma = 3\ (003)_1/(22\bar{1})_2$, 109.47°/[1$\bar{1}$0] boundary in aluminium. A units are indicated in this and following figures by full lines. (111) planes in the upper and lower grains are seen to be inclined by 54.74° to the boundary.

Figure 3 shows the relaxed structure of the $\Sigma = 9$ boundary. A suitable B unit, occupying half a period of this centred boundary is shown by broken lines. Again each unit of this boundary may be associated formally with a lattice dislocation of Burgers vector 2[111].

Figures 4*a*, *b* show the relaxed structure and hydrostatic stress field map of the $\Sigma = 97$ boundary. Although the units are distorted, two A units, shown by full lines, and one B unit, shown by broken lines, may be readily identified in every half period of this centred boundary. The corresponding decomposition of each half period vector of this boundary is as follows:

$$\tfrac{1}{4}[17, 17, 2]_1 = \tfrac{2}{2}[330]_1 + \tfrac{1}{4}[552]_1,$$

$$\tfrac{1}{4}[\bar{7}, \bar{7}, \bar{22}]_2 = \tfrac{2}{2}[\bar{1}\bar{1}4]_2 + \tfrac{1}{4}[\bar{3}\bar{3}6]_2.$$

The stress field of an edge g.b.d. is centred at each B unit, again shown by broken lines in figure 4*b*. One $(002)_1$ plane and three $(44\bar{2})_2$ planes are shown in figure 4*a* entering the boundary and terminating at a B unit. These terminating planes correspond to a g.b.d. of total Burgers vector $[001]_1$ (or $\frac{1}{3}[22\bar{1}]_2$). The most appropriate g.b.d. description of this boundary is that using the $\Sigma = 3\ (003)_1/(22\bar{1})_2$ reference structure, because in that case B units are located at the cores of $[001]_1$ (non-primitive) $\Sigma = 3$ d.s.c. dislocations. There is a one-to-one correspondence between this secondary g.b.d. description and the stress field map of the boundary, figure 4*b*.

Each grain contributes an equal amount to the 'extra material' associated with each $[001]_1$ g.b.d. and this is consistent with the absence of steps in the boundary plane. The spacing of these dislocations is a half period of the $\Sigma = 97$ boundary and with use of Frank's formula it can be verified that they accommodate the 9.51° deviation from the exact $\Sigma = 3$ misorientation.

Figures 5*a*, *b* show the relaxed structure and hydrostatic stress field map of the $\Sigma = 11$ boundary. Every period of this non-centred boundary is composed of two B units, shown by

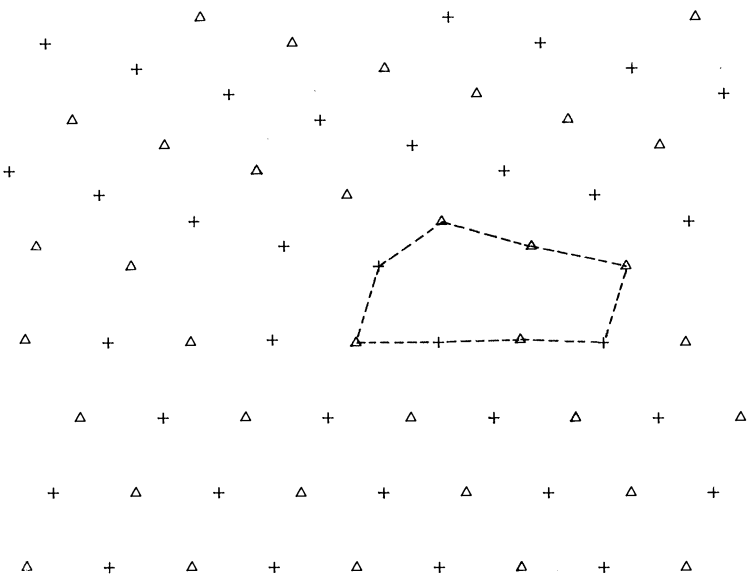

FIGURE 3. Relaxed structure of $\Sigma = 9$ $(\bar{1}\bar{1}5)_1/(33\bar{3})_2$, 141.06°/$[1\bar{1}0]$ boundary in aluminium. B units are indicated in this and following figures by broken lines.

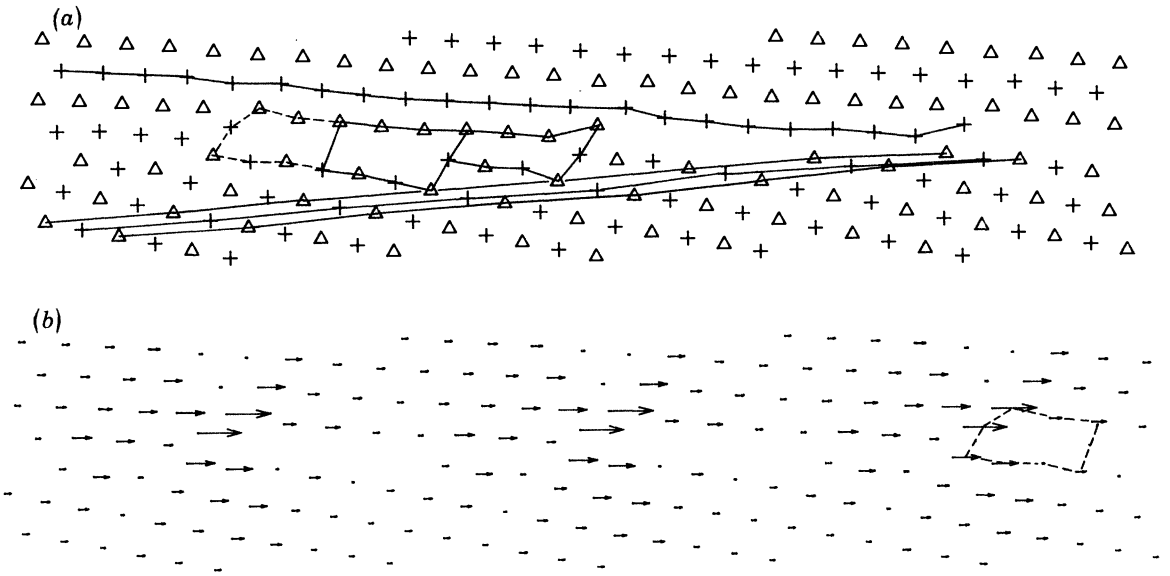

FIGURE 4. (*a*) Relaxed structure of $\Sigma = 97$ $(\bar{1}, \bar{1}, 17)_1/(11, 11, \bar{7})_2$, 118.98°/$[1\bar{1}0]$ boundary in aluminium. One $(002)_1$ plane and three $(44\bar{2})_2$ planes are shown entering the boundary and terminating at a B unit. (*b*) Corresponding hydrostatic stress field map.

broken lines, and one A unit, shown by full lines. Again, the units are distorted but nevertheless identifiable. The decomposition of the upper and lower period vectors is thus

$$[441]_1 = \tfrac{2}{4}[552]_1 + \tfrac{1}{2}[330]_1,$$

$$[\overline{225}]_2 = \tfrac{2}{4}[\overline{336}]_2 + \tfrac{1}{2}[\overline{114}]_2.$$

In figure 5*b* it is seen that A units are located at the centres of edge g.b.d. stress fields. The most appropriate g.b.d. description is therefore that using the $\Sigma = 9\,(\overline{1}\overline{1}5)_1/(33\overline{3})_2$ reference structure. In that case the edge g.b.d. stress fields at A units are caused by $-\frac{2}{9}[\overline{1}\overline{1}5]_1$ (or $-\frac{2}{3}[11\overline{1}]_2$) non-primitive $\Sigma = 9$ d.s.c. dislocations. One $(11\overline{1})_2$ plane and three $(\overline{1}\overline{1}5)_1$ planes are shown in figure 5*a* entering the boundary and terminating at an A unit. Both grains contribute an equal amount to the 'extra material' associated with each $-\frac{2}{9}[\overline{1}\overline{1}5]_1$ dislocation, which is consistent with the absence of steps in the boundary plane. The spacing of the dislocations is one period of the $\Sigma = 11$ boundary and using Frank's formula it can be verified that they accommodate the $-11.54°$ deviation from the $\Sigma = 9$ orientation.

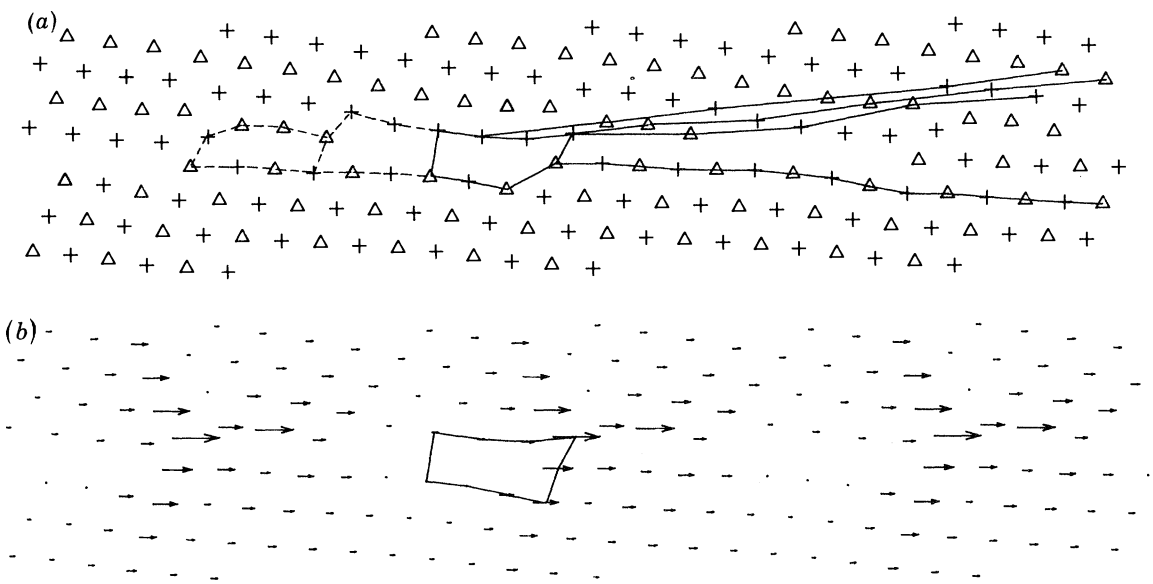

FIGURE 5. (*a*) Relaxed structure of $\Sigma = 11\ (\overline{1}\overline{1}8)_1/(55\overline{4})_2$, $129.52°/[1\overline{1}0]$ boundary in aluminium. One $(11\overline{1})_2$ and three $(\overline{1}\overline{1}5)_1$ planes are shown entering the boundary and terminating at an A unit. (*b*) Corresponding hydrostatic stress field map.

The $\Sigma = 41$ boundary is the 1:1 boundary of this series. Between this and the $\Sigma = 3$ boundary orientations there are more A than B units and the most appropriate g.b.d. description uses the $\Sigma = 3\,(003)_1/(22\overline{1})_2$ reference structure. Similarly the most appropriate structure between the $\Sigma = 41$ and $\Sigma = 9$ boundary orientations is the $\Sigma = 9\,(\overline{1}\overline{1}5)_1/(33\overline{3})_2$ boundary. These g.b.d. descriptions are equally appropriate at the $\Sigma = 41$ boundary. Figures 6*a*, *b* show the relaxed structure and hydrostatic stress field map of the $\Sigma = 41$ boundary. Each half period of this centred boundary is composed of one A unit (full lines) and one B unit (dashed lines). Figure 6*b* indicates that every half period of this boundary contains one edge dislocation and that these dislocations are localized and physically distinct. These dislocations may either be regarded as

$[001]_1/(\frac{1}{3}[22\bar{1}]_2)$ preserving the $\Sigma = 3$ favoured boundary, or as $-\frac{2}{9}[\bar{1}\bar{1}5]_1$ $(-\frac{2}{3}[11\bar{1}]_2)$ preserving the $\Sigma = 9$ boundary.

In aluminium $\Sigma = 9\,(\bar{1}\bar{1}5)_1/(33\bar{3})_2$ and $\Sigma = 3\,(003)_1/(22\bar{1})_2$ are favoured boundaries because their units are the fundamental structural elements of the intervening $\xi = 1$ boundary structures.

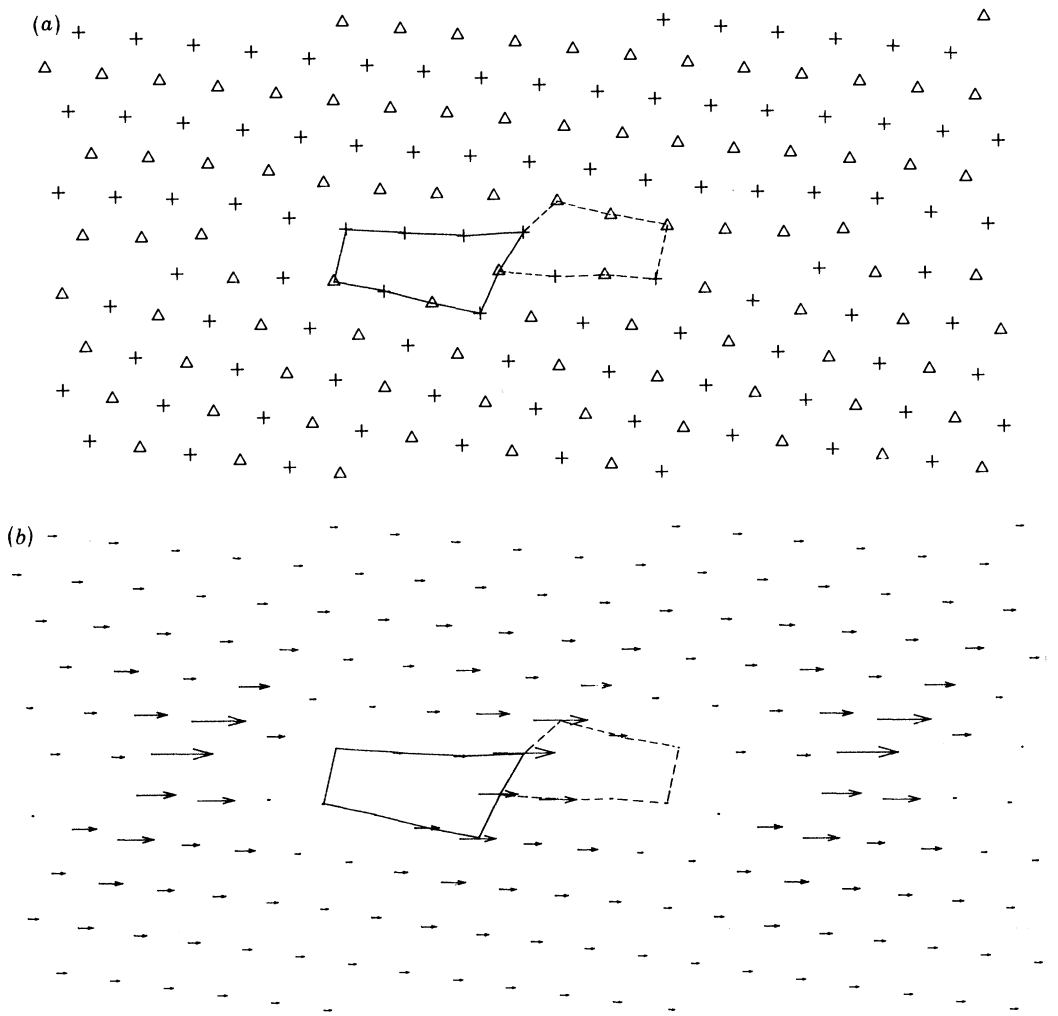

FIGURE 6. (*a*) Relaxed structure of $\Sigma = 41\ (\bar{1}, \bar{1}, 11)_1/(77\bar{5})_2$, $124.12°/[1\bar{1}0]$ boundary in aluminium. (*b*) Corresponding hydrostatic stress field map.

On the basis of the above calculations it seems very likely that all $\xi = 1$ boundaries in aluminium, in the misorientation range $109.47 < \theta < 141.06°$, are composed of A and B units from these favoured boundaries. Continuity of boundary structure (see part I, §4.3) therefore probably exists throughout this misorientation range. The unit representation of any boundary in this range may be deduced in precisely the same way as shown in part I, §4.3. For example, consider $\Sigma = 1193\,(\bar{7}, \bar{7}, 59)_1/(37, 37, \bar{2}\bar{9})_2$, $128.52°/[1\bar{1}0]$ in aluminium. The upper and lower grain period vectors are $\boldsymbol{p}_1 = \frac{1}{2}[59, 59, 14]_1$ and $\boldsymbol{p}_2 = \frac{1}{2}[\bar{2}\bar{9}, \bar{2}\bar{9}, \bar{7}\bar{4}]_2$ respectively. To find the numbers, x and y, of A and B units in each half period of this centred boundary we express the half period vectors as linear combinations of vectors characterizing A and B units:

$$\tfrac{1}{4}[59, 59, 14]_1 = \tfrac{1}{2}x[330]_1 + \tfrac{1}{4}y[552]_1, \quad \tfrac{1}{4}[\bar{2}\bar{9}, \bar{2}\bar{9}, \bar{7}\bar{4}]_2 = \tfrac{1}{2}x[\bar{1}\bar{1}4]_2 + \tfrac{1}{4}y[\bar{3}\bar{3}6]_2.$$

Solving either of these equations we find $x = 4$ and $y = 7$. Using continuity of boundary structure, as shown in part I, §4.3, we find that the unit representation of the boundary is

$$|\mathrm{ABBABBABBAB.ABBABBABBAB}|.$$

Since A units are in the minority in this case it is appropriate to associate each A unit with the core of $-\frac{2}{9}[\bar{1}\bar{1}5]_1$ (or $-\frac{2}{3}[11\bar{1}]_2$) secondary dislocation, preserving the $\Sigma = 9$ favoured boundary structure.

3.3 *Faceting of* $[1\bar{1}0]$ *tilt boundaries in the* $\Sigma = 3$ *coincidence system*

Before the results of the calculations are presented we would like to point out the limitations of simulating equilibrium faceting in atomistic studies. First, if a boundary has a tendency to facet, the lengths of the facets are artificially constrained owing to the use of periodic border conditions parallel to the macroscopic boundary plane. This means that any facets introduced during the relaxation will be repeated periodically with the period of the original boundary plane. In this case the interaction energies between the boundary facets may represent a significant contribution to the total energy, and thereby influence which facets are formed. Furthermore, in such calculations a symmetrical $[1\bar{1}0]$ tilt boundary is constrained to remain symmetrical even if there is a tendency for it to facet into asymmetrical tilt boundaries. This is because the period vectors of symmetrical $[1\bar{1}0]$ tilt boundaries are always smaller than the period vectors of any asymmetrical $[1\bar{1}0]$ tilt boundaries in the same coincidence system. Therefore it is highly unlikely that equilibrium faceting, as given by the Wulff construction, will be obtained when periodic border conditions are used. On the other hand it is possible to take advantage of the constraints imposed by the periodic border conditions, and to carry out the Wulff construction for the energies of certain boundaries possessing the same value of Σ, and thereby deduce the equilibrium faceting behaviour. This is the approach adopted in this work. The calculations were performed with use of the potential for copper and although several $\Sigma = 3$ boundaries have been studied previously with the potential for aluminium (Pond & Vitek 1977) these calculations have not been extended further. The reason is that boundary energies may be evaluated precisely when the potential for copper is used, because it is short range. This is in contrast to the potential for aluminium which is long range and oscillatory, so that precise evaluation of corresponding boundary energies requires consideration of a very large number of neighbours (see for example Vitek 1975).

TABLE 3

boundary	mean boundary plane	energy/(mJ/m²)
$(111)_1/(\bar{1}\bar{1}1)_2$	(001)	22
$(003)_1/(22\bar{1})_2$	(111)	2878
$(115)_1/(33\bar{3})_2$	(221)	1111
$(112)_1/(11\bar{2})_2$	(110)	838

The relaxed structure and energy of the ten smallest-period $\Sigma = 3[1\bar{1}0]$ tilt boundaries throughout the 90° inclination range, have been calculated. The four smallest-period boundaries did not undergo faceting during the relaxation, either because it was not energetically favourable for them to facet, or because the periodic border constraints inhibited their faceting. The relaxed structures of the remaining six boundaries appeared to contain facets from the four smallest-period boundaries. It is therefore very likely that the four smallest-period boundaries are the only four possible singular interfaces appearing in the equilibrium Wulff shape.

The relaxed structures and energies of the symmetrical tilt boundaries are virtually identical to those presented by Crocker & Faridi (1980), who used the same interatomic potential. The high energy of the $(112)_1$ boundary was commented on in detail in that paper. Figures 7 and 8 show the relaxed structures of the $(003)_1/(22\bar{1})_2$ and $(115)_1/(33\bar{3})_2$ boundaries.

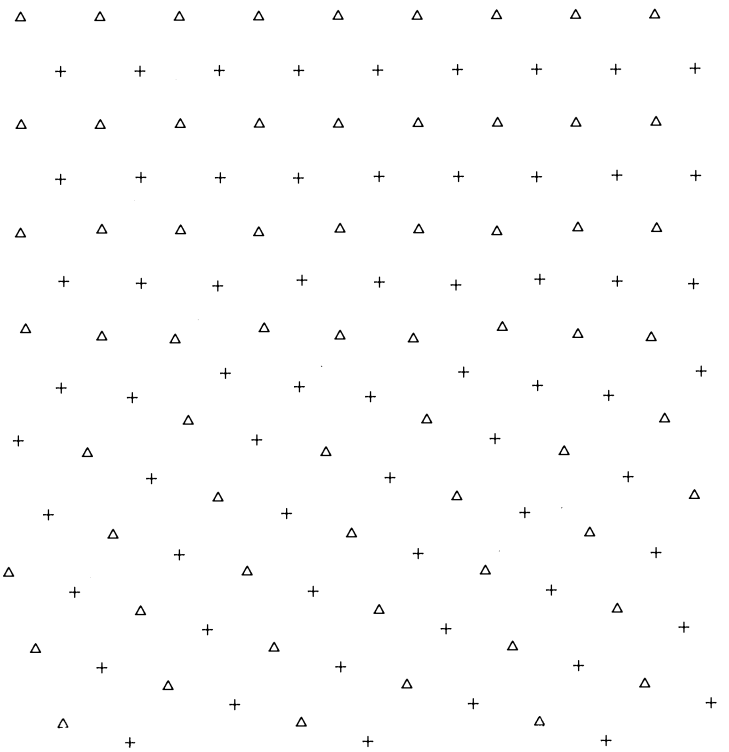

FIGURE 7. Relaxed structure of $\Sigma = 3\ (003)_1/(22\bar{1})_2$, $70.53°/[1\bar{1}0]$ boundary calculated with the potential for copper.

FIGURE 8. Relaxed structure of $\Sigma = 3\ (115)_1/(33\bar{3})_2$, $70.53°/[1\bar{1}0]$ boundary calculated with the potential for copper.

PHILOSOPHICAL TRANSACTIONS OF THE ROYAL SOCIETY A MATHEMATICAL, PHYSICAL & ENGINEERING SCIENCES

If the mean boundary plane is (hhk) the corresponding boundary is represented on a polar Wulff plot by a radius vector, whose length is proportional to the energy of the boundary, and which makes an angle of arctan (k/h) to the x-axis. In this way the above four boundaries are represented in the first quadrant of the polar Wulff plot shown in figure 9. The axes of the plot shown in figure 9 are mirror planes of the Wulff plot because they correspond to (110) and (001) mean boundary planes. It is therefore sufficient to consider only one quadrant of the plot. The equilibrium Wulff shape is shown by broken lines. This is the equilibrium Wulff shape of an infinitely long prism grain in the $\Sigma = 3$ orientation with the surrounding grain. The axis of the

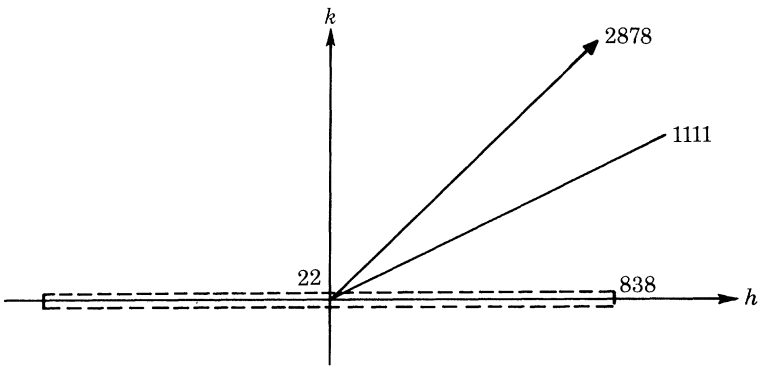

FIGURE 9. Wulff construction for $\Sigma = 3$ $[1\bar{1}0]$ tilt boundaries with use of boundary energies obtained with the potential for copper. The axes are mirror planes of the plot. The equilibrium Wulff shape is shown by the broken lines.

prism is parallel to $[1\bar{1}0]_1$ and the faces of the prism are $(111)_1/(\bar{1}\bar{1}1)_2$ and $(112)_1/(11\bar{2})_2$ symmetrical tilt boundaries, and their variants. This indicates that all asymmetrical $\Sigma = 3$ $[1\bar{1}0]$ tilt boundaries, calculated with the potential for copper, tend to facet into the two symmetrical tilt boundaries. The ratio of the lengths of the coherent facet to the incoherent facet in an equilibrated prism is about 38.

4. Discussion

In §2 it was shown that all tilt boundaries, with the same tilt axis, may be classified by two parameters: Σ and ξ. The parameter ξ is determined by the mean boundary plane, i.e. the plane of the ideal crystal that is obtained when the misorientation of boundaries in that ξ-system tends to zero. Since all boundaries in a ξ-system share the same mean boundary plane, ξ varies with the inclination of the two grains and not their misorientation. On the other hand Σ varies only with the misorientation of the two grains and not their inclination. Therefore Σ and ξ are independent parameters that, for a given tilt axis, may be used to specify a tilt boundary uniquely. The significance of this classification is that it indicates which tilt boundaries to choose to study equilibrium faceting or intrinsic secondary g.b.ds. Equilibrium faceting introduces boundary units from the same coincidence system, i.e. Σ = constant but ξ varies. Intrinsic secondary g.b.d. stress fields accompany the introduction of boundary units belonging to the same ξ-system, i.e. ξ = constant but Σ varies. Systematic studies of these two modes of decomposition may then be made by either computer simulation or experiments. The underlying physical assumptions are that the mean boundary plane changes only by the formation of perfect steps and that intrinsic g.b.ds, accommodating a misorientation from some reference structure, are never associated

with steps. For reasons of energetics (King & Smith 1980, King 1982) the latter assumption is expected to be valid for almost all cases.

A general tilt boundary may undergo both faceting and intrinsic secondary g.b.d. formation to minimize the interfacial energy. This would introduce boundary units belonging to lower-index mean boundary planes and characteristic of boundaries with possibly lower values of Σ.

Although this classification has only been illustrated for the $[1\bar{1}0]$ tilt axis it may be readily generalized to any tilt axis in any cubic Bravais lattice. In general if the tilt axis is $\boldsymbol{t} = [UVW]$ we choose two orthogonal primitive lattice vectors, $\boldsymbol{u}_1$ and $\boldsymbol{u}_2$, in the zone of $\boldsymbol{t}$. The period vectors, $\boldsymbol{p}_1$ and $\boldsymbol{p}_2$, in the upper and lower grains of $[UVW]$ tilt boundaries with mean period vector parallel to $\boldsymbol{u}_1$ are written as follows

$$\boldsymbol{p}_1 = x\boldsymbol{u}_1 + y\boldsymbol{u}_2, \quad \boldsymbol{p}_2 = x\boldsymbol{u}_1 - y\boldsymbol{u}_2, \tag{5}$$

where x and y are integers. The mean boundary plane normal is then parallel to $\boldsymbol{u}_2$. We may write $\boldsymbol{u}_2$ as $f[-(Vk+Wl), Uk, Ul]$, where f is the appropriate cell factor and k and l are integers. All $[UVW]$ tilt boundaries, with mean boundary plane $(-(Vk+Wl), Uk, Ul)$, may, by convention, be assigned to the ξ-system $\xi = l/k$. From equation (5) we obtain

$$\tan \tfrac{1}{2}\theta = y|\boldsymbol{u}_2|/x|\boldsymbol{u}_1|.$$

Since $\boldsymbol{u}_1 = \boldsymbol{u}_2 \wedge \boldsymbol{t}$, and all three vectors are orthogonal, we may write $|\boldsymbol{u}_1| = |\boldsymbol{u}_2|\,|\boldsymbol{t}|$ and therefore $\tan \tfrac{1}{2}\theta = y/(x(U^2+V^2+W^2)^{\frac{1}{2}})$. This is the usual expression for $\tan \tfrac{1}{2}\theta$ obtained originally by Ranganathan (1966) for c.s.ls generated by rotations about $\langle UVW \rangle$.

Asymmetrical tilt boundaries of the $\xi = 1$ system in aluminium were shown in § 3.2 to conform to precisely the same scheme of favoured and non-favoured boundaries as developed in part I for symmetrical tilt boundaries. Thus $\Sigma = 3\,(003)_1/(22\bar{1})_2$, $109.47°/[1\bar{1}0]$ and $\Sigma = 9\,(\bar{1}\bar{1}5)_1/(33\bar{3})_2$, $141.06°/[1\bar{1}0]$ are favoured boundaries and the intervening $\xi = 1$ non-favoured boundaries are composed of units from these favoured boundaries. Therefore the boundary structure changes continuously in this misorientation range enabling us to predict the unit representation of any $\xi = 1$ boundary in this range. Intrinsic secondary g.b.d. stress fields are, again, located at the intermittences of the sequence of majority units in the boundary. Hence the most appropriate reference structure for the secondary g.b.d. description is again the favoured boundary composed of the majority units. The hydrostatic stress field maps reveal that the secondary intrinsic g.b.ds are localized and distinct. It may be concluded that the answers provided in part I, § 7 to the questions raised in part I, § 1 are equally applicable to asymmetrical tilt boundaries.

In part I and § 3.2 of this paper the Burgers vector of intrinsic secondary g.b.ds, accommodating a misorientation from some favoured boundary reference structure, was always the smallest possible d.s.c. vector that did not require steps in the favoured boundary plane. For example, in part I, § 4.2 $\frac{2}{27}[115]_1$ non-primitive $\Sigma = 27$ d.s.c. dislocations preserve the $\Sigma = 27\,(115)_1$ favoured boundary. One $\{115\}$ plane originating from each grain terminates at every $\frac{2}{27}[115]_1$ dislocation core and hence each grain 'contributes' $\frac{1}{27}[115]_1$ to the total Burgers vector. We may generalize this result. Consider a favoured tilt boundary $(h_1k_1l_1)_1/(h_2k_2l_2)_2$ in a simple cubic Bravais lattice. The plane indices are expressed in a form such that $h_1^2+k_1^2+l_1^2 = h_2^2+k_2^2+l_2^2$ and there is no factor common to all six indices. In addition, if there is no common factor in either h_1, k_1, l_1 or h_2, k_2, l_2 then both grains contribute $x(h_1^2+k_1^2+l_1^2)^{-\frac{1}{2}}$ to the total intrinsic secondary dislocation Burgers vector magnitude of $2x(h_1^2+k_1^2+l_1^2)^{-\frac{1}{2}}$. Here x is the smallest integer such that the total Burgers vector, $2x(h_1^2+k_1^2+l_1^2)^{-1}[h_1k_1l_1]_1$, is a d.s.c. vector of the coincidence

system to which the favoured boundary belongs. Now suppose that h_2, k_2, l_2 do share a common factor n. Then

$$h_1^2+k_1^2+l_1^2 = n^2(h_2'^2+k_2'^2+l_2'^2);$$

e.g. $(221)_1/(003)_2$, for which $n = 3$, $h_2' = 0$, $k_2' = 0$, $l_2' = 1$. In that case both grains contribute $x(h_2'^2+k_2'^2+l_2'^2)^{-\frac{1}{2}}$ in magnitude to the total Burgers vector $2x(h_2'^2+k_2'^2+l_2'^2)^{-1}[h_2'k_2'l_2']_2$, where x has the same meaning as before. This means that each dislocation is associated with $nx(h_1k_1l_1)_1$ plane terminations from the upper grain and $x(h_2'k_2'l_2')$ plane terminations from the lower grain. The same procedure may be applied to f.c.c. and b.c.c. Bravais lattices except that the interplanar spacing must be correctly adjusted to correspond to planes containing atoms. For example, suppose $\Sigma = 3(114)_1/(330)_2$ is favoured in some f.c.c. metal. The interplanar spacing in the lower grain is three times as large as in the upper grain: $n = 3$. But the planes parallel to the boundary containing atoms are $(228)_1$ and $(220)_2$. Therefore $h_2' = 2$, $k_2' = 2$, $l_2' = 0$. One plane termination in the lower grain contributes $8^{-\frac{1}{2}}$ and three plane terminations in the upper grain contribute $3\times(72)^{-\frac{1}{2}} = 8^{-\frac{1}{2}}$ to the total Burgers vector $\frac{1}{6}[114]_1/\frac{1}{2}[110]_2$. Since this vector is a $\Sigma = 3$ d.s.c. vector, $x = 1$. The Burgers vectors of intrinsic secondary dislocations do not always have to be non-primitive d.s.c. vectors. For example, if $\Sigma = 9(114)_1/(\bar{1}\bar{1}4)_2$, $38.94°/[1\bar{1}0]$ were favoured in some f.c.c. metal it would be preserved by $\frac{1}{18}[114]_1/\frac{1}{18}[\bar{1}\bar{1}4]_2$, which are primitive $\Sigma = 9$ d.s.c. dislocations.

It is instructive to apply the above considerations of intrinsic secondary dislocation Burgers vectors to the Burgers vectors of lattice dislocations in low-angle tilt boundaries. Consider low-angle $[1\bar{1}0]$ tilt boundaries with mean boundary plane (111) in an f.c.c. crystal. As the misorientation angle tends to zero the boundary plane tends to (111) of the ideal crystal. Following the above procedure we find that the smallest Burgers vector of lattice dislocations that preserves the (111) plane of the ideal crystal, without introducing steps or stacking faults, is $\boldsymbol{b} = 2[111]$. It will be recalled that this is the Burgers vector of primary dislocations associated formally with each unit of the favoured boundaries in the $\xi = 1$ study. However, it would seem very improbable that a low angle asymmetrical tilt boundary with (111) mean boundary plane would contain lattice dislocations with Burgers vector $2[111]$. Indeed any very low angle ($\theta < 1°$ say) tilt boundary must consist of well separated lattice dislocations. It is well known that two sets of edge lattice dislocations are required to produce a low-angle asymmetrical tilt boundary. The two sets of dislocations do not truly lie in a plane because of local interactions, which tend to make the dislocations lie along a line inclined at 45° to their Burgers vectors (Hirth & Lothe 1968). The presence of intrinsic g.b.ds with Burgers vector components parallel to the boundary is contrary to the assumptions made in this paper. We therefore envisage that as the misorientation of a tilt boundary increases, the constituent lattice dislocations interact eventually to form units of some 'high' angle tilt boundary in the same ξ-system. Such a transition may be thought of as the transition from the low- to the high-angle régime and could conceivably occur quite abruptly (i.e. discontinuously) at a certain misorientation that depends on the ξ-system.

In §3.3 it was pointed out that relaxation methods using periodic border conditions will generally produce metastable structures of asymmetrical tilt boundaries that are not singular interfaces of the corresponding Wulff shape. The use of periodic border conditions imposes an artificial constraint on the size of the facets. For a symmetrical tilt boundary, with the periodic cell equal to one period of the boundary, no faceting can take place because all other tilt boundaries, within the same coincidence system, have longer periods. However, as shown in §3.3, it is possible to use this deficiency to deduce the equilibrium shape of an embedded prism grain

bounded by tilt boundaries parallel to the prism axis. The equilibrium shape is determined by the Wulff construction, as shown in §3.3. The energies of relaxed tilt boundaries that do not appear to facet are plotted on a Wulff plot. The relaxed structures of other tilt boundaries, in the same coincidence system, are checked to ensure that they exhibit some tendency to facet into those interfaces entered on the Wulff plot. The equilibrium Wulff shape is then derived by the usual polar Wulff construction, taking into account only the limited number of points in the Wulff plot. In this way it was found that only symmetrical $\Sigma = 3[1\bar{1}0]$ tilt boundaries, calculated with the potential for copper, are stable with respect to faceting. Thus, only those boundaries, and their crystallographic variants, may be favoured. To show that they are indeed favoured boundaries it is necessary to show that their units are among the fundamental structural elements of boundaries nearby in the misorientation range within their respective ξ-systems.

Recently Brokman *et al.* (1981) concluded that probably all asymmetrical tilt boundaries in cubic crystals facet into whole units of symmetrical tilt boundaries. The faceting was described as 'atomistic' because it was repeated in each period of the original asymmetrical tilt boundary, and was thus on an atomistic scale. In §2 it was shown that such decompositions can certainly take place, provided, of course, symmetrical tilt boundaries exist with the tilt axis under consideration. The condition for the existence of symmetrical tilt boundaries is that the tilt axis lies in a ⟨100⟩ or ⟨110⟩ zone. However, there is no *a priori* reason why it should be energetically favourable for all asymmetrical tilt boundaries to facet into symmetrical tilt boundaries when it is geometrically possible. Because equilibrium faceting behaviour is determined by considerations of energetics only, the Wulff construction can indicate which are the stable facets. Faceting of a non-equilibrium interface will always tend to occur into stable facets. While the Wulff construction does not take into account the interaction energy between adjacet facets we know that this energy is positive. Therefore the stable facets will tend to maximize their sizes subject to kinetic constraints. In addition, it is reiterated that the simulation of faceting of tilt boundaries will always produce perfect steps in the interface, because of the requirement of zero stresses far from the boundary. Faceting involving imperfect steps may be studied atomistically only by imposing the elastic field of the g.b.ds, associated with the steps, far from the boundary. This is the method used, for example, in studies of imperfect steps in {112} twin boundaries in b.c.c. metals (Yamaguchi & Vitek 1976, Bristowe & Crocker 1977) and extrinsic grain boundary dislocations (Sutton *et al.* 1979). Since the step vector of an imperfect step is not a c.s.l. vector it does not characterize a unit of any tilt boundary.

This research has been supported by the National Science Foundation through the MRL Program, contract no. DMR79-23647.

References

Ashby, M. F. 1972 *Surf. Sci.* **31**, 498.
Bristowe, P. D. & Crocker, A. G. 1977 *Acta metall.* **25**, 1363.
Brokman, A., Bristowe, P. D. & Balluffi, R. W. 1981 *Scr. metall.* **15**, 201.
Christian, J. W. 1975 *The theory of transformations in metals and alloys*, p. 37. Oxford: Pergamon Press.
Christian, J. W. & Knowles, K. M. 1981 *Proc. conf. on phase transformations*, Pittsburgh. New York: A.I.M.E.
Crocker, A. G. & Faridi, B. A. 1980 *Acta metall.* **28**, 549.
Fortes, M. A. 1972 *Rev. fis. Quim. Engen.* **4**A, 7.
Hirth, J. P. & Balluffi, R. W. 1973 *Acta metall.* **21**, 929.
Hirth, J. P. & Lothe, J. 1968 *Theory of dislocations*, p. 645. New York: McGraw-Hill.
King, A. H. 1982 *Acta metall.* **30**, 419.

PHILOSOPHICAL TRANSACTIONS OF THE ROYAL SOCIETY A MATHEMATICAL, PHYSICAL & ENGINEERING SCIENCES

King, A. H. & Smith, D. A. 1980 *Acta crystallogr.* A **36**, 335.
Pond, R. C. & Vitek, V. 1977 *Proc. R. Soc. Lond.* A **357**, 453.
Ranganathan, S. 1966 *Acta crystallogr.* **21**, 197.
Sleeswyk, A. W. 1962 *Acta metall.* **10**, 705.
Sutton, A. P., Smith, D. A. & Vitek, V. 1979 *J. Microsc.* **116**, 97.
Vitek, V. 1975 *Scr. metall.* **9**, 611.
Yamaguchi, M. & Vitek, V. 1976 *Phil. Mag.* **34**, 7.

Appendix

Consider a periodic grain boundary that may be tilt, twist or mixed character. Let the indices of the boundary plane with respect to the upper and lower grains be $(h_1k_1l_1)_1$ and $(h_2k_2l_2)_2$ respectively. The condition for the boundary to be periodic is

$$h_1^2+k_1^2+l_1^2 = h_2^2+k_2^2+l_2^2. \tag{A 1}$$

In general, the indices will not be coprime. If h_1, k_1 and l_1 share a common factor m and h_2, k_2 and l_2 share a common factor n then the condition for the boundary to be periodic becomes

$$m^2(H_1^2+K_1^2+L_1^2) = n^2(H_2^2+K_2^2+L_2^2), \tag{A 2}$$

where H_1, K_1 and L_1 are coprime and H_2, K_2 and L_2 are coprime. Given the odd/even form of the indices h_1, k_1 and l_1 we enquire whether there is any restriction on the odd/even form of the indices h_2, k_2 and l_2 to satisfy equation (A 1). In addition we shall show that both m and n in equation (A 2) must be odd.

There are three possible combinations of odd and even integers for the coprime triplet (H, K, L), namely (odd, odd, even), (odd, even, even) and (odd, odd, odd). A cyclic permutation of any one of these is regarded as the same as that one, e.g. (odd, even, even) is the same as (even, odd, even). Consider the squares of all integers modulo 8. Any even number squared is congruent to 0 or 4 mod 8. Any odd number squared is congruent to 1 mod 8. If equation (A 2) is satisfied it must also be satisfied modulo any integer. The following analysis examines both sides of equation (A 2) modulo 8 for the three possible forms of $(H_1K_1L_1)$. The various possibilities are summarized in the table below.

form of $(H_1K_1L_1)$	$(H_1^2+K_1^2+L_1^2)$ mod 8	$m^2(H_1^2+K_1^2+L_1^2)$ mod 8	
		n even	n odd
(odd, odd, odd)	3	0 or 4	3
(odd, even, even)	1 or 5	0 or 4	1 or 5
(odd, odd, even)	2 or 6	0 or 4	2 or 6

We see that if equation (A 2) is satisfied modulo 8 then the form of $(H_1K_1L_1)$ must be the same as the form of $(H_2K_2L_2)$ and in addition m and n must both be odd. Therefore the forms of $(h_1k_1l_1)$ and $(h_2k_2l_2)$ must also be the same.